Contrast Gain Control Is Drift-Rate Dependent: An Informational Analysis

M. A. Hietanen, N. A. Crowder and M. R. Ibbotson

J Neurophysiol 97:1078-1087, 2007. First published Nov 22, 2006; doi:10.1152/jn.00991.2006

J Neurophysiol 97: 1078–1087, 2007.
First published November 22, 2006; doi:10.1152/jn.00991.2006.

Contrast Gain Control Is Drift-Rate Dependent: An Informational Analysis

M. A. Hietanen, N. A. Crowder, and M. R. Ibbotson
Visual Sciences, Research School of Biological Sciences, Australian National University, Canberra, Australia

Submitted 17 September 2006; accepted in final form 17 November 2006

Hietanen MA, Crowder NA, Ibbotson MR. Contrast gain control is drift-rate dependent: an informational analysis. *J Neurophysiol* 97: 1078–1087, 2007. First published November 22, 2006; doi:10.1152/jn.00991.2006. Neurons in the visual cortex code relative changes in illumination (contrast) and adapt their sensitivities to the visual scene by centering the steepest regions of their sigmoidal contrast response functions (CRFs: spike rate as a function of contrast) on the prevailing contrast. The influence of this contrast gain control has not been reported at nonoptimal drift rates. We calculated the Fisher information contained in the CRFs of halothane-anesthetized cats. Fisher information gives a measure of the accuracy of contrast representations based on the ratio of the square of the steepness of the CRF and the spike-rate dependency of the spiking variance. Variance increases with spike rate, so Fisher information is maximal where the CRF is steep and spike rates are low. Here, we show that the contrast at which the maximal Fisher information (C_{MFI}) occurs for each adapting drift rate is at a fixed level above the adapting contrast. For adapting contrasts of 0 to 0.32 the relationship between C_{MFI} and adapting contrast is well described by a straight line with a slope close to 1. The intercept of this line on the C_{MFI}-axis is drift-rate dependent, although the slope is not. At high drift rates relative to each cell's peak the C_{MFI} offset is higher than that for low drift rates. The results show that the contrast coding strategy in visual cortex maximizes accuracy for contrasts above the prevailing contrast in the environment for all drift rates. We argue that tuning the system for accuracy at contrasts above the prevailing value is optimal for viewing natural scenes.

INTRODUCTION

Stimulus contrast is arguably the most fundamental stimulus parameter that influences the responses of single cells in the primary visual cortex (Hubel and Wiesel 1962; Movshon et al. 1977). Response amplitudes are dependent on stimulus contrast in a sigmoidal fashion when plotted against log-contrast, such that there is one component in the middle of the curve that is very steep before response saturation (solid lines, Fig. 1*A*). Prolonged exposure to visual patterns causes these contrast response functions (CRFs) to shift along the contrast axis (Albrecht et al. 1984; 2002; Bonds 1991; Carandini and Ferster 1997; Movshon and Lennie 1979; Ohzawa et al. 1985; Sclar et al. 1989). For example, in Fig. 1*A* compare the fitted line through the open circles (nonadapted) with that fitted to the filled circles (adapted). These lateral shifts are referred to as contrast gain control. The CRFs are also compressed in many cases, such that the postadaptation asymptote of the spiking rate is lower than that in the nonadapted case (Fig. 1*A*; cf. Albrecht et al. 1984). This latter effect is referred to as response gain control. The functional role attributed to contrast gain control is that it keeps the most sensitive part of the contrast response function centered on the prevailing environmental contrast, which allows efficient neural coding (for review, see Ibbotson 2005a).

It is well known that adaptation is pattern selective (Carandini et al. 1997; Dragoi et al. 2000; Movshon and Lennie 1979; Müller et al. 1999). For example, in many cortical cells contrast gain control is observed only when the spatial frequencies of the adapting and test stimuli are similar (Movshon and Lennie 1979). That contrast adaptation is selective for spatial frequency was also shown perceptually using psychophysics (Blakemore et al. 1973; Snowden and Hammett 1996). This spatial-frequency–selective effect cannot be explained by general changes in sensitivity but rather by some spatial-frequency–specific mechanism. Visual scenes are usually in motion as the result of eye and body movements or external movements in the environment (Clifford and Ibbotson 2002). Therefore the influence of image speed on contrast gain control must be important (Ibbotson 2005b). Speed is calculated by dividing the drift rate by spatial frequency. Because it is established that adaptation is spatial frequency selective, it is also important to look at the drift-rate selectivity of the effect.

Maddess et al. (1988) conducted experiments in which moving gratings were presented to the receptive fields of cortical cells at a range of drift rates for 6.7 s. They used the ratio between the initial response and the final response in this time window to assess what parameters governed the decline in response over time as their measure of adaptation. They showed that in some cells there was little adaptation at low drift rates but profound adaptation at high drift rates, whereas in others marked adaptation occurred for all drift rates. Statistical analysis showed that the direction of motion and drift rate were the primary parameters governing adaptation, whereas other stimulus parameters, such as contrast, spatial frequency, and ocular dominance, were of less importance. Saul and Cynader (1989a,b) found that adaptation at peak drift rates and spatial frequencies led to the largest reductions in response gain when subsequent test stimuli were presented at the same frequencies. However, neither of these studies looked for the effect of drift rate specifically on contrast coding because contrast was not altered either throughout the stimulus period (Maddess et al. 1988) or between the adaptation and test phases of the experiments (Saul and Cynader 1989a,b). Thus although we know that drift rate is important in governing response decay over time, it is not clear how the drift rate during adaptation specifically influences subsequent contrast coding.

Here we use a protocol in which we adapted and tested at a range of contrasts and drift rates to assess how drift rate and

Address for reprint requests and other correspondence: M. R. Ibbotson, Visual Sciences, Research School of Biological Sciences, Australian National University, Canberra, ACT, Australia 2601 (E-mail: Ibbotson@rsbs.anu.edu.au).

The costs of publication of this article were defrayed in part by the payment of page charges. The article must therefore be hereby marked "*advertisement*" in accordance with 18 U.S.C. Section 1734 solely to indicate this fact.

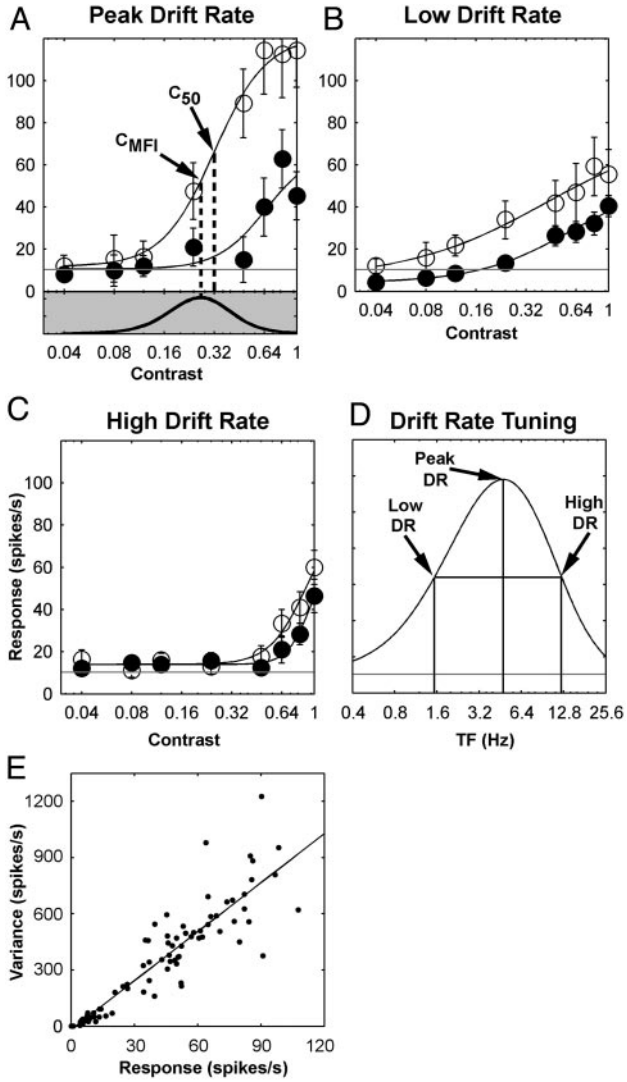

FIG. 1. Contrast response functions (CRFs) from an example cell showing the adaptation effects of adapting and testing at: peak drift rate (*A*), low drift rate (*B*), and high drift rate (*C*). Adaptation and test drift rates were determined from the drift-rate response function for the cell (arrows in *D*). *A–C*: CRFs obtained after adaptation to 0 contrast are indicated with open circles, whereas those obtained after adaptation to 0.32 contrast are indicated with solid circles. Error bars: ± SE. *A*: shift in the CRF to higher contrasts after peak drift-rate adaptation. *B*: similar shifts after adaptation at low drift rates. *C*: nonadapted CRF has its range at higher contrasts when tested at high rather than low drift rates. Adaptation at high drift rates moves the CRF toward higher contrasts. *E*: plot of the relationship between response and the variance of the response for a single example cell calculated using drift rate and contrast tuning trials. Solid line shows the line of best fit through the data points ($R^2 = 0.81$).

contrast interact. We select drift rates for each cell that cover its full tuning range. Moreover, we use a different method of analysis from that classically used to assess changes in contrast coding after adaptation. We use Fisher information to measure the neural accuracy in coding contrast by taking account of the steepness of the contrast response functions and the variance in the spiking responses of the cells. Fisher information was previously used as a measure of the accuracy of sound level estimation in guinea pigs (Dean et al. 2005) and as a factor for calculating speed discriminability in primate extrastriate cortex (Nover et al. 2005). Fisher information is comparable to stimulus-specific information when calculated from a large population of neurons (Butts and Goldman 2006). Fisher information, a measure of how accurately a stimulus is represented, was previously shown to influence the upper bound of the discrimination of two closely spaced stimuli (Nover et al. 2005; Pouget et al. 1998; Seung and Sompolinsky 1993). As in previous studies we found that variance increases in visual cells as the spike rate increases (e.g., Clifford and Ibbotson 2000; Tolhurst et al. 1981). Thus maximum Fisher information and thus the most accurate discriminations between contrasts occur where spike rates are low and the contrast response functions are steep. We calculate the Fisher information in the entire population of our recorded cells, thus offering quantitative population data for future modeling efforts. Importantly, we find that the maximum information occurs at a contrast given by the adapting contrast plus a constant additional value (offset). On average, the offset between adapting contrast and the contrast at which maximum information content occurs is drift-rate dependent.

METHODS

Physiological preparation

Experimental procedures were approved by the Animal Experimentation Ethics Committee of the Australian National University and were previously described in detail (Crowder et al. 2006). Briefly, after surgery under anesthesia with ketamine HCl (20 mg/kg, administered intramuscularly; Ilium, Smithfield, NSW, Australia), lacquer-coated tungsten microelectrodes were placed in either area 17 or area 18 of the cat's cortex. Anesthesia and neuromuscular blockade were maintained using 0.5% gaseous halothane and gallamine triethiodide (10 mg · kg^{-1} · h^{-1}). Animals were ventilated with a 2:1 ratio of N_2O and O_2. Corrective lenses focused the stimulus on the retina at a distance of 57 cm in front of the animal. Then 3-mm-diameter artificial pupils were placed in front of the eyes. Extracellular signals from individual units were acquired with a CED1401 interface and Spike2 software sampled at 40 kHz (Cambridge Electronic Designs, Cambridge, UK).

Stimuli

The dominant eye and receptive field location of each neuron were initially determined using a hand-driven light bar. The nondominant eye was covered and quantitative testing was performed on the dominant eye with visual stimuli produced by a VSG Series 2/5 stimulus generator (Cambridge Research Systems, Cambridge, UK) and presented on a calibrated monitor (Eizo T662-T, 100-Hz refresh, 1,024 × 768 pixels). The location and size of the classical receptive field (RF), as well as the preferred orientation/direction, spatial frequency (SF), and drift rate (DR) were determined by calculating on-line tuning functions for each stimulus parameter. RFs were located within 15° of visual angle from area centralis. The starting phase of the grating was randomized on a trial-by-trial basis, so that drift rates <2 Hz still had their full cycles displayed, albeit averaged across trials rather than within a trial. The adapting stimulus and that for measuring contrast response functions constituted an optimally oriented sine-wave grating (optimal spatial frequency) presented in a circular aperture the size of the classical RF. The aperture had a diameter of 0.5–10° and was surrounded by a gray of mean luminance (*Lum*; 50 cd/m^2). Sine-wave contrast is defined as

$$\text{Michelson contrast} = \frac{Lum_{max} - Lum_{min}}{Lum_{max} + Lum_{min}}$$

In the initial adaptation phase a grating at the adaptation contrast and drift rate was presented for 30 s. Contrast response functions were collected by presenting each contrast (0.04–1) in random order for 0.5-s tests (10 repetitions) interleaved with either 4 s of mean luminance (adaptation to 0 contrast) or 4 s of the adaptation grating

(adaptation to 0.08, 0.16, or 0.32 contrast). A 3-min recovery period was allowed between collecting the data for every contrast response function. Firing rates used to construct contrast response functions were calculated by taking the mean firing rate across repeats from 0.1 to 0.5 s after the test stimuli appeared.

Quantitative analysis

DRIFT RATE. Drift-rate tuning was determined by presenting a grating moving at 10 drift rates, each repeated 12 times, covering an appropriate range of drift rates for the cell being tested (usually 0.38–48.0 Hz). Drift rates were presented in random order and each grating was presented for 1 s and was followed by 4 s at mean luminance. The three adaptation/test drift rates used were determined by examining the nonadapted drift rate tuning function and selecting the drift rate at which peak firing occurred, as well as the two drift rates that elicited 50% of the maximum response. These values are shown as arrows in Fig. 1*D*. Drift-rate tuning functions were fit with a skewed Gaussian function using the equation

$$R_x = R_{\max} \exp\left\{ - \left[\frac{\log (x/x_{\text{peak}})}{\text{B} + \text{A} \log (x/x_{\text{peak}})} \right]^2 \right\} + R_{Spont}$$

where R_x is the response at drift rate x, $R_{\max}$ controls the amplitude, x_{peak} is the cell's preferred drift rate at which the peak spiking rate $R_{\max}$ occurs, A controls the skew of the curve, and B is the bandwidth. R_{Spont} is the measured spontaneous activity and was not allowed to vary as part of the least-squares fitting routine. Goodness of fit to the curve was measured with R^2 values and across all fits this measure formed a highly skewed distribution with a median of 0.94.

CONTRAST. In agreement with previous studies, the contrast response functions collected in the present study were suitably described by a sigmoid function (Fig. 1*A*; Sclar et al. 1989). Sigmoid curves were fit using the equation

$$\text{R}(c) = \frac{R_{\max} \times c^{\text{n}}}{c^{\text{n}} + C_{50}^{\text{n}}} + M$$

where R(c) is the amplitude of the evoked response at contrast c, M is the spontaneous rate, n is the exponent that determines the steepness of the curve, $R_{\max}$ is the maximum elevation in response above the spontaneous rate, and C_{50} is the contrast that generates a response elevation of half $R_{\max}$. Goodness of fit to the curve was measured with R^2 values and across all fits this measure formed a highly skewed distribution with a median of 0.94. In cases where contrast response functions did not show saturation at higher contrasts the upper and lower $R_{\max}$ bounds for the fit were set at ±10% of the maximum measured neuronal response above spontaneous, as measured for the most responsive condition.

FISHER INFORMATION. We adapted the formulae relating to Fisher information from Nover et al. (2005) and Dean et al. (2005) and applied them to contrast response functions. We calculated Fisher information as a function of contrast using

$$F_i(c) = \frac{\left[\frac{\partial R_i(c)}{\partial c} \right]^2}{kR_i(c)} T$$

where $F_i(c)$ is the Fisher information for a single neuron i, when tested at contrast c; T is the length of time the test contrast was present; and k is a constant calculated as the ratio of spiking variance to the spiking rate and was determined using linear regression of each cell's responses to all tests conducted on that cell. An example of this relationship for one cell is shown in Fig. 1*E*. Because information from multiple independent sources can be thought of as additive, the total Fisher information for our population of neurons as a function of contrast is given by

$$F(c) = \sum_{i=1}^{N} \frac{\left[\frac{\partial R_i(c)}{\partial \text{c}} \right]^2}{\text{k}R_i(c)} 0.4$$

The above formula assumes that the spiking noise between neurons is not correlated and that the cells are independent. Given that this assumption is likely to be false (Kohn and Smith 2005; Shadlen and Newsome 1998; Zohary et al. 1994) our estimation of the total Fisher information at the population level will be liberal. However, this is not important in the current context because we are interested in relative, rather than absolute, changes in accuracy.

Because not all conditions had identical sample sizes all population results are presented as averages across cells. Fisher information in this case is measured in units of nats · s^{-1} · $cell^{-1}$ because it is an average measure across cells and nats/s is bits/s in natural log units. From Fisher information curves of this type, the contrast at which maximum Fisher information (C_{MFI}) occurred was obtained and used as a measure to compare across stimulus conditions. Although C_{MFI} is a useful measure, it is important to note that the shape of the entire Fisher information curve is important.

Histology

Electrode tracks were reconstructed and track locations and depths were verified using established procedures (Crowder et al. 2006; Price et al. 2006).

RESULTS

We recorded from 139 units in cat visual cortex, 86 in area 17 and 53 in area 18. Thirty-two cells were classed as simple and 107 as complex. No differences were found between the different cell groups with respect to the properties investigated here, so the data from all cells were combined in the population analysis. Cells were first tested for their drift-rate dependency (see METHODS), from which we extracted the peak drift rate and the two points at which the response was half the amplitude of the peak response (relative to the mean spontaneous rate). The peak, low, and high drift rates are marked with arrows and vertical lines in Fig. 1*D*.

Adapt and test at the same drift rates

We recorded contrast response functions (CRFs) after adaptation to four contrasts (0, 0.08, 0.16, and 0.32) at peak, low, and high drift rates (Fig. 1). After exposure to zero contrast, tests at all drift rates produced sigmoidal CRFs. The tests at high drift rates always produced curves that were displaced rightward relative to those for lower drift rates (compare the open circles in Fig. 1, *A* and *B* with Fig. 1*C*). After adaptation with a fixed contrast, the contrast response functions of most cells moved rightward and downward regardless of the drift rate (filled circles, Fig. 1).

It is typical to use the value of C_{50} obtained from the fits to the CRFs to assess where the steep part of the curve occurs (Albrecht et al. 1984). C_{50} is the contrast that generates half the asymptotic firing rate and can be regarded as the semisaturation point (see METHODS). The C_{50} is marked on the nonadapted CRF in Fig. 1*A*. In Fig. 2 each row shows histograms of the C_{50} values for all cells after adaptation to one of four contrasts (0, 0.08, 0.16, and 0.32). The *left*, *middle*, and *right columns* in Fig. 2 show the data when the adapting and test drift rates were at the peak, low, and high values, respectively. For all drift rates, increases in adapting contrast lead to increases in the

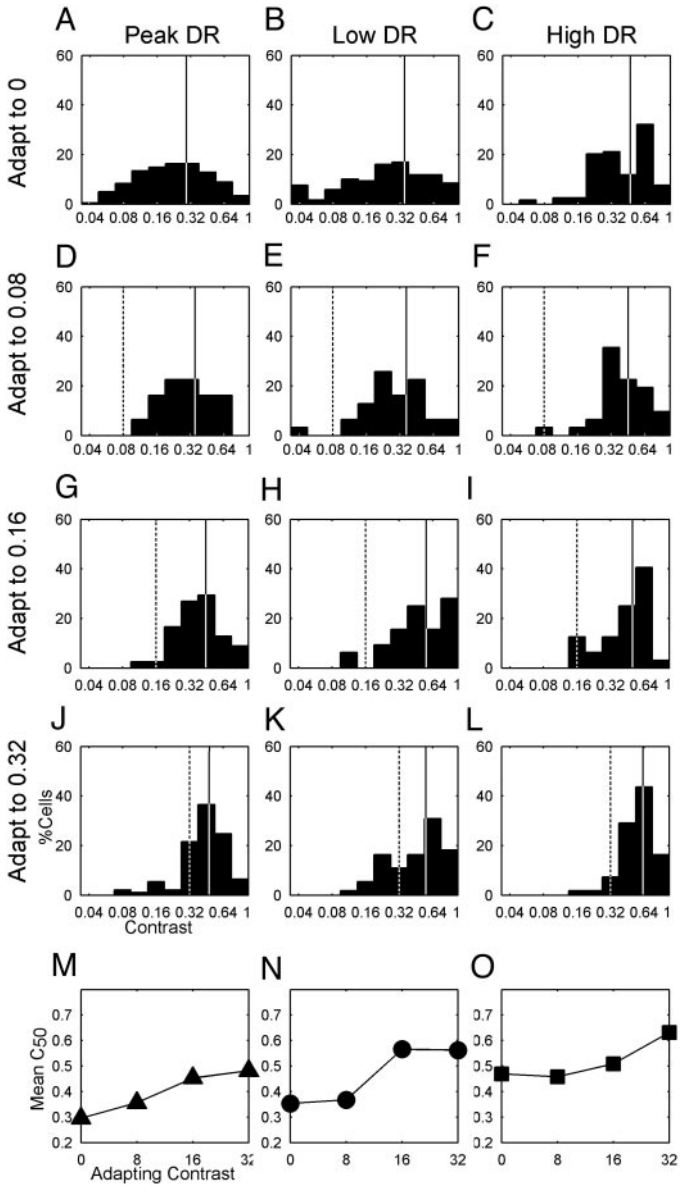

FIG. 2. Population histograms showing the C_{50} values (contrast at which half the maximum firing rate occurs in the CRF) of the cells after adaptation at: peak (*A*, *D*, *G*, *J*); low (*B*, *E*, *H*, *K*); and high (*C*, F, *I*, *L*) drift rates. Adapting contrast (0, 0.08, 0.16, or 0.32) is shown with a vertical dashed line and the population mean is shown with a solid vertical line. As the adapting contrast increases, so do the C_{50} values (compare solid lines down a column). Adaptation to nonpeak drift rates showed higher C_{50} values than adaptation to peak drift rate, with adaptation to a high drift rate showing the largest C_{50} values (compare solid lines across a row). *M*, *N*, *O*: mean C_{50} of the population at each adaptation contrast after adaptation at peak, low, and high drift rates, respectively.

mean of the C_{50} distribution. Vertical dashed lines indicate the adaptation contrast and vertical solid lines the population mean. Graphs at the bottom of each column in Fig. 2 plot this relationship and reveal the clear upward trend in mean C_{50} as adapting contrast increases.

Analysis using a repeated-measures ANOVA revealed a main effect of both adapting contrast ($F = 44.6$, $P \ll 0.01$) and adapting drift rate ($F = 22.3$, $P \ll 0.01$). Given the significant interaction between adapting contrast and drift rate ($F = 2.1194$, $P < 0.05$), post hoc comparisons revealed that after both adaptation to low and peak drift rates, as we increased adaptation contrast C_{50} also increased ($P < 0.01$). Conversely, after high drift-rate adaptation increasing the adaptation contrast did not always lead to a significant increase in C_{50} ($P > 0.05$).

Using C_{50} demonstrates a clear adaptive effect, although the analysis is limited because it reduces a complex sigmoidal curve to a single semisaturation parameter. Thus much of the detail in the contrast coding system is lost, such as the steepness of slopes and the amount of variance in the data. Consequently, we used a measure of the Fisher information for each CRF to assess how information across all contrasts changed after adaptation. As an example, the Fisher information curve obtained after adaptation to zero contrast (for a single cell) is shown in the gray box below Fig. 1*A*. It is clear that there is a wide range of contrasts where substantial Fisher information is available. The contrast at which maximum Fisher information (C_{MFI}) was obtained is marked by a vertical line that passes through the peak of the information curve (Fig. 1*A*). The contrasts at which the C_{MFI} and the C_{50} values occurred were strongly correlated ($R^2 = 0.98$), with MFIs always occurring at lower contrasts than the C_{50} (Fig. 3). The mean difference in contrast between the two measures was 0.08 (SD 0.015).

Population information code for contrast

Average population Fisher information was calculated by taking the total Fisher information (see METHODS) for all of the cells for each experimental condition and dividing by the number of cells. The average Fisher information curves for all adapting drift rates for the population are presented in Fig. 4, following the same format as that in Fig. 2. As adapting contrast increased, the entire Fisher information distribution moved to higher contrasts. It is evident from Fig. 4 that C_{MFI}

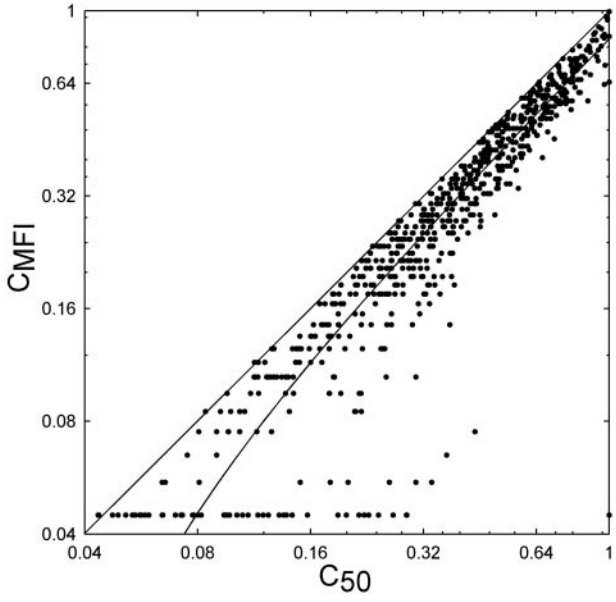

FIG. 3. Scatterplot showing the relationship between C_{50} and C_{MFI} [contrast at which the maximum Fisher information (MFI) occurs] for every cell and every test. Solid diagonal line shows the line of equality. Solid curved line shows the best fit to the data using linear regression. In every case the C_{MFI} was a lower contrast than C_{50}, with the 2 measures being highly correlated ($R^2 = 0.98$).

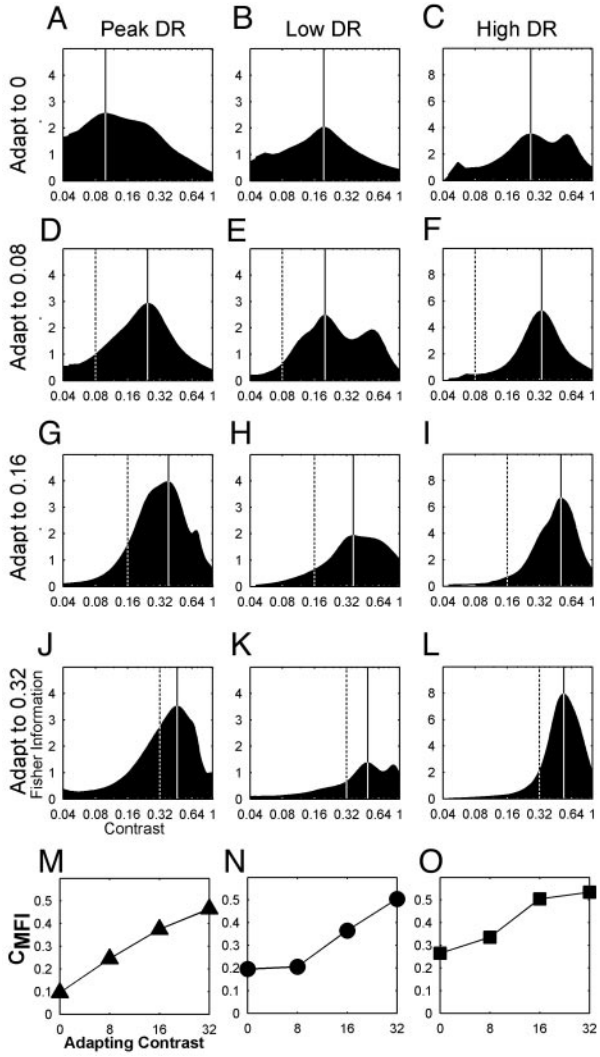

FIG. 4. Population Fisher information curves after adaptation at: peak (*A*, *D*, *G*, *J*), low (*B*, *E*, *H*, *K*), and high (*C*, *F*, *I*, *L*) drift rates. Adapting contrast (0, 0.08, 0.16, or 0.32) is shown with a vertical dashed line. Solid lines correspond to the contrast of MFI. As adapting contrast increased, the Fisher information curve generally moved to higher contrasts. For most adaptation contrast/drift rates the Fisher information began to increase close to the adapting contrast. Fisher information was greatest when adapted and tested at high drift rates (note ordinate change in *C*, *F*, *I*, *L*). *M*, *N*, *O*: contrast at which the maximum Fisher information occurred (C_{MFI}) of the population at each adaptation contrast after adaptation at peak, low, and high drift rates, respectively.

does not occur at the adapting contrast. That is, maximum information is not optimized to coincide with the prevailing stimulus contrast. Interestingly, Fisher information generally began to increase at contrasts just below the adapting contrast, peaked at a contrast higher than the adaptation contrast, and remained elevated for most contrasts above the adapting contrast.

For all adapting contrasts and drift rates, C_{MFI} occurs at a value well above the adapting contrast. In Fig. 5 we present plots of C_{MFI} as functions of adapting contrasts for each of the adapting drift rates. All of the relationships have been fitted with linear functions. Linear fits through the data points are excellent, with R^2 values of 0.84–0.94. The slopes of the four curves are also similar (low drift rate, 1.05; peak drift rate, 1.13; high drift rate, 0.88). Thus the lines run approximately parallel to each other. For low and peak drift rates, the fitted lines are offset vertically from the line passing through the adapting contrasts by values of 0.171 and 0.137, respectively. For the tests at high drift rates the offset is larger: 0.287. Thus for any given adapting contrast the C_{MFI} is given by the adapting contrast (AC) plus a fixed offset value (OS): C_{MFI} = AC + OS. Importantly, for a given drift rate OS is constant. Thus we conclude that the absolute value of C_{MFI} is drift-rate dependent.

Adapt and test at different drift rates

In the previous experiments, it was not possible to determine whether the spike rate in response to the test stimuli is dictated by the adaptation drift rate alone or whether the test drift rate also affects the response. To address this issue, we adapted at low and tested at high drift rates or adapted at high and tested at low drift rates. The question being addressed was whether a constant adapting contrast leads to the same changes in Fisher information when the adaptation and test drift rates differed at a single adapting contrast (0.32).

Figure 6*A* shows the Fisher information of the cell population after adaptation to zero contrast, with tests at low drift rates (Note: *A*, *B*, *E*, and *F* in Fig. 6 are repeated from *B*, *C*, *K*, and *L* in Fig. 4, respectively) and C_{MFI} occurs at a low contrast of 0.195. After adaptation to a high drift rate the C_{MFI} shifts upward to 0.455 (Fig. 6*C*). After adaptation to a low drift rate the Fisher information at contrasts <0.32 drops out significantly and the C_{MFI} is 0.505 (Fig. 6*E*). Figure 6*B* shows the Fisher information for the population with adaptation at zero contrast and at high drift rates. Fisher information occurred over a wide range from 0.2 to

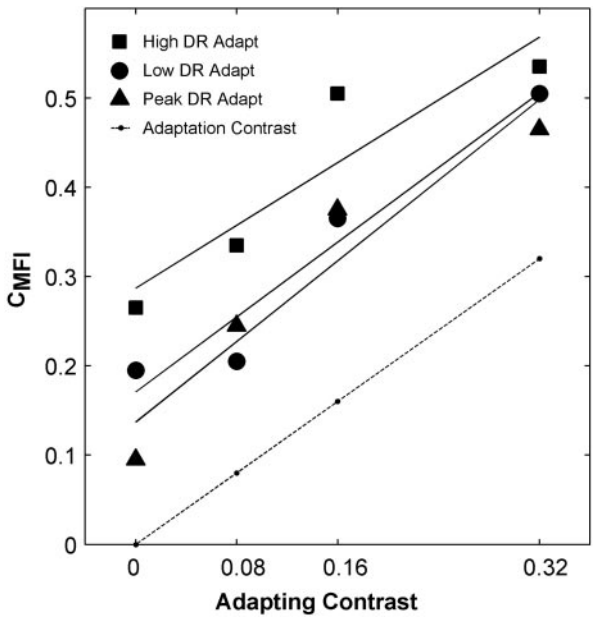

FIG. 5. Contrast at which maximum Fisher information occurred (C_{MFI}) as a function of adapting contrasts for peak (square), low (circle), and high (triangle) adapting drift rates. Lines indicate a linear fit (R^2 values >0.84). For comparison a line through the adaptation contrasts is also presented (dots). Slopes of the 4 lines are very similar. Low and peak drift-rate adaptations produce similar C_{MFI} values. High drift-rate adaptation tends to produce C_{MFI} values at higher contrasts. This difference indicates that contrast adaptation is drift-rate dependent.

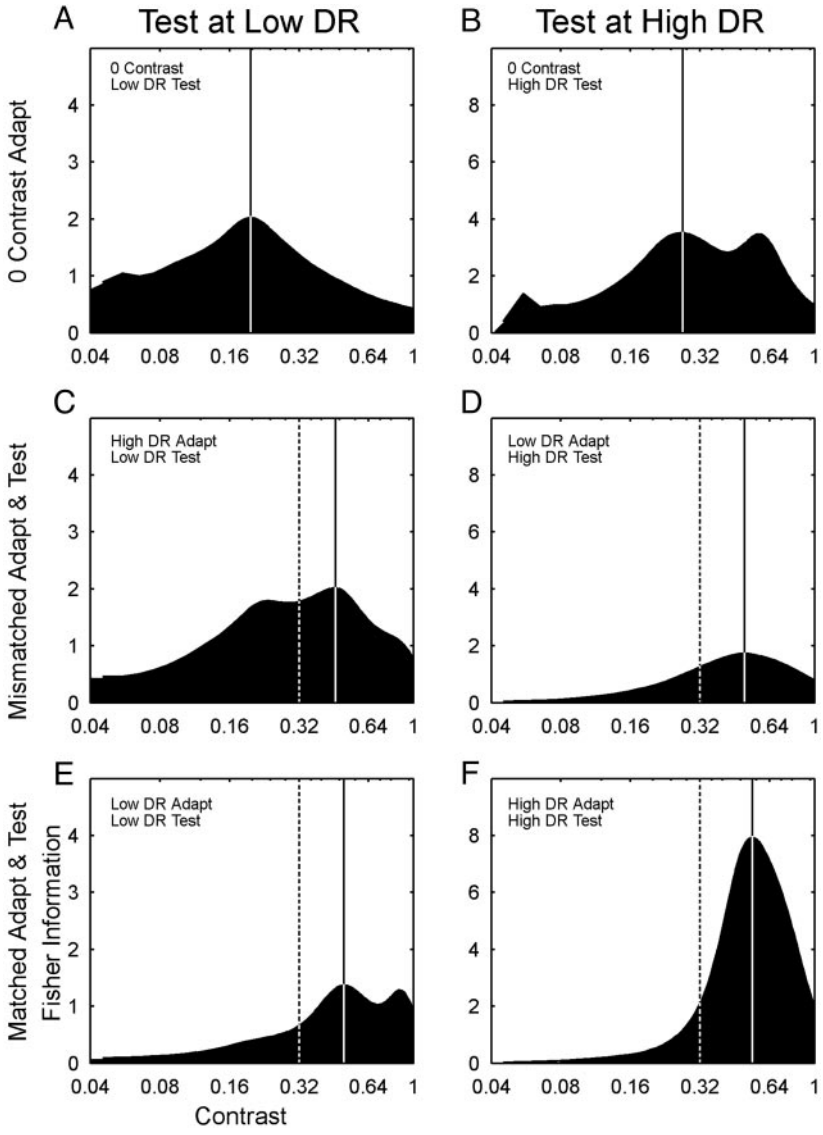

FIG. 6. Population Fisher information curves tested at low (*A*, *C*, *E*) and high (*B*, *D*, *F*) drift rates. Adapting contrast (0, 0.32) is shown with a vertical dashed line. Solid lines correspond to the contrast at which maximum Fisher information occurred (C_{MFI}). Experiment compared: unmatched adaptation at high and testing at low drift rates (*C*); unmatched adaptation at low and testing at high drift rates (*D*); matched adaptation and test drift rates [low adapt, low test (*F*)]; matched adaptation and test [high adapt, high test (*E*)]. Adaptation moves the Fisher information curves to higher contrasts and there is virtually no difference between the C_{MFI} for matched and unmatched conditions. When adapting at low and testing at high drift rates there is an overall decrease in the Fisher information at the adaptation contrast. When adapting at high and testing at low drift rates the Fisher information at the adaptation contrast increases. Adaptation at low drift rates reduces the amplitude of Fisher information more than adaptation at high drift rates.

0.7, with the C_{MFI} at 0.265 (Fig. 6*B*). After adaptation to low drift rates the C_{MFI} shifted upward to 0.495 and the amount of Fisher information fell quite dramatically (Fig. 6*D*). After adaptation at the same high drift rates the C_{MFI} shifts upward to a contrast of 0.535 and total information increases considerably as a result of steepening of the CRFs and relatively low spike rates (Fig. 6*F*). These results show that adapting drift rate, rather than test drift rate, has a profound effect on the amount of Fisher information present in the CRF regardless of the subsequent drift rate.

Adapting drift rates

Figure 7 shows the actual drift rates used in the experiments for all cells. Means of the distributions for the low (*A*), peak (*B*), and high (*C*) drift rates were 1.1, 5.5, and 13.9 Hz. The high drift-rate values can be regarded as the 50% cutoff values for the tuning functions of the cells. For comparison with cells that provide the feedforward input to the primary visual cortex we have included arrows indicating the peak drift rates for X-type (Fig. 7*B*, solid arrow) and Y-type (Fig. 7*B*, open arrow) cells from the dorsal lateral geniculate nucleus (dLGN) of the cat [from Saul and Humphrey (1990)]. The dLGN cells were tested with a contrast of 0.4, which is similar to the adapting contrast of 0.32 used in most of our experiments.

Comparing cortical cell types and areas

We compared the distributions of C_{MFI} after peak, low, and high drift-rate adaptation for simple versus complex cells and found that there was no significant difference between them (*t*-test, $P > 0.05$). Simple and complex cells were distinguished based on their F1/F0 ratio. This was measured in standard preliminary trials in which the phase of the sinusoidal gratings was constant from trial to trial. F1 is the amplitude of the fundamental response and F0 is the mean time-averaged response of the neuron (Crowder et al. 2006; Ibbotson et al. 2005). Ratios greater than unity indicated simple cells, whereas cells with ratios below unity were classed as complex. A similar comparison between area 17 and 18 cells also showed no significant differences (*t*-test, $P > 0.05$).

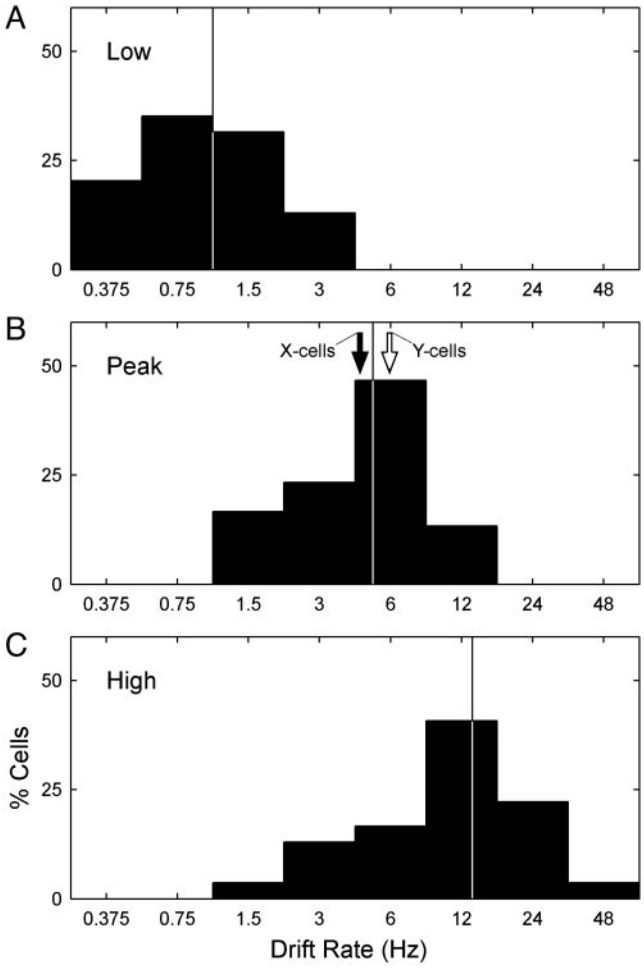

FIG. 7. Histograms of the drift rates [temporal frequencies (TFs)] used to adapt the cells. *A*: drift rates at the lower 50% of maximum response mark. *B*: drift rates at which the peak response occurred. *C*: drift rates at the higher 50% of the maximum response mark. Vertical lines indicate the mean drift rates in each condition for the population. Also shown are the mean peak drift rates obtained from X-type (solid arrow) and Y-type (open arrow) dorsal lateral geniculate nucleus cells, taken from Saul and Humphrey (1990).

DISCUSSION

Functional implications of contrast adaptation

In cats, cortical neurons that are tested at peak drift rates after exposure to a zero contrast stimulus have contrast response functions with semisaturation values (C_{50}) that occur at a range of values, but they are most common at low contrasts of around 0.1 (e.g., Albrecht and Hamilton 1982; Chirimuuta et al. 2003). For a population of nonadapted cat cortical neurons we get a distribution of C_{50} values (Fig. 2*A*) that appreciably overlap with those reported by previous experimenters. Chirimuuta et al. (2003) showed that the distribution of nonadapted C_{50} values in cat cortex matched the distribution of contrasts in natural scenes, which peaks just below a contrast of 0.1. They suggest through their analysis that C_{50} is a good measure for use in comparing cortical function with natural scenes, at least without prior adaptation. Chirimuuta et al. (2003) suggest that adaptation to gratings with contrasts chosen in proportion to their occurrence in natural scenes might "tighten up" the distribution of C_{50} values so that they center more accurately on the adapting value. We did not specifically tailor our adapting stimuli to those found in natural scenes but we did explore how closely the distributions of C_{50} matched a single adapting contrast. We found that C_{50} did not provide a good match to the adapting contrast at any adapting contrast or drift rate. In virtually all cells, C_{50} moved to contrasts above the adapting contrast.

A problem exists in trying to match values of C_{50} to the prevailing contrast in a scene because, in effect, it is trying to fit just one point on a sigmoidal curve to scenes with complex contrast profiles. Instead, in the present work we used Fisher information as a measure of the information accuracy within the contrast response functions of each cell. Fisher information takes account of the steepness of the contrast response functions (CRFs) and the variance in the data. There is a clear relationship between firing rate and variance such that the higher the firing rate, the greater the variance (Fig. 1*E*). This fact poses a problem for the nervous system because as firing rates approach the peak in a tuning function the accuracy of the measurement declines. Therefore for a CRF with the same difference in firing rates between two contrasts, the accuracy of responses at high contrasts is poor, whereas the accuracy at lower contrasts is relatively high. Fisher information is thus maximal where the steepness of the CRF is high but the variance is small. This point occurs early on the rising phase of the CRF (Fig. 1*A*). This coding strategy is interesting because it predicts that maximum Fisher information can be derived from lower than maximal firing rates and thus lower levels of energy consumption. Thus adjusting the location on the contrast axis where maximum information accuracy occurs may not only benefit contrast coding but should also assist in reducing overall energy consumption in the cortex (Attwell and Laughlin 2001). Estimates suggest that only one cortical neuron in 63 could be active at 50 spikes/s based on the human brain's normal energy consumption (Lennie 2003), and reducing firing rates through adaptation makes this estimate seem more plausible.

It is well established that cortical neurons adjust their sensitivity to contrasts based on the prevailing contrast in the environment (e.g., Ohzawa et al. 1985). In this way, it is thought that cells maximize their capacity to discriminate between contrasts close to the most common value in the scene. In the present work we used Fisher information to see how cells optimize their tuning functions such that the least variable and most useful (in terms of contrast discriminability) region of the tuning functions changes after adaptation. Surprisingly, we found that the contrast at which the maximum Fisher information (C_{MFI}) occurs does not correspond to the prevailing contrast. We found that the C_{MFI} occurs at a constant positive contrast offset from the adapting contrast for a wide range of adapting values (0–32% contrast). Thus the maximum amount of information in the population code is at a contrast 15–30% higher than the adapting contrast. Thus the cell population appears to be optimally tuned to discriminate about contrasts higher than the prevailing environmental conditions.

Why would the information accuracy be maximal at contrasts above the prevailing contrast instead of at the prevailing contrast? We suggest the following example. Imagine the receptive field of a cortical neuron that is exposed to a relatively unchanging image, e.g., a field of grass. Our data show that adaptation would shift the CRF of that cell such that the

maximum Fisher information would occur at a higher contrast than the mean contrast of the background. Thus firing rates to the prevailing contrast would be low, which is efficient in terms of both data transmission and energy conservation. Virtually any object that passes through the receptive field of the neuron (such as a bird flying over the grass) will have a different luminance profile than the prevailing background. The leading edge of the object will thus generate a relatively high contrast border as it moves through the receptive field. Given that adaptation to the background has increased the contrast at which maximum information is available, the cell will respond with the most accurate signal possible and allow for enhanced discrimination between the object and the environment. However, an object with a contrast profile similar to that of the environment (camouflage) would be poorly distinguishable as long as it is not in motion. Moreover, because firing rates that correlate to the maximum Fisher information are low, the response will also be energy efficient (Lennie 2003).

The relationship between C_{MFI} and adapting contrast is linear and has the same slope at low, peak, and high drift rates across the cell population. However, although the slope of the relationship is the same, the absolute shift in C_{MFI} is higher for high drift rates. This result indicates that contrast adaptation is drift-rate dependent. Movshon and Lennie (1979) showed that contrast adaptation was dependent on spatial frequency. Only when the spatial frequencies of the adapting and test stimuli were similar did contrast gain control occur, although this is not the case for all cortical neurons (e.g., see DISCUSSION in Ohzawa et al. 1985). Maddess et al. (1988) suggested that drift rate is one of the primary stimulus determinants governing adaptation. However, this study investigated the decline in firing rate over only the first few seconds of stimulation with a moving grating in which all the stimulus parameters were kept constant throughout. There was no attempt to see what affect the response decline had on the contrast coding to subsequently presented stimuli. Saul and Cynader (1989b) also showed that the drift rate of an adapting grating was important in determining the amplitudes of responses to subsequently presented stimuli. Maximal response attenuation occurred after adaptation to a grating moving at the same drift rate as the subsequent test grating. Although our results suggest a small absolute dependency of the amount of contrast gain control on drift rate, adaptation leads to a similar general effect at all drift rates: enhanced information at contrasts above the prevailing contrast in the scene.

The finding that drift rate is important to the mechanism of contrast adaptation is reinforced by the results in Fig. 6. It is evident that adaptation at low drift rates, regardless of the subsequent test drift rate (Fig. 6, *D* and *E*), generates an overall reduction in the information content (area under the graphs) than with no prior exposure to contrast (Fig. 6, *A* and *B*). Conversely, adaptation at high drift rates, regardless of the test drift rate, tends to increase the area under the information curve (Fig. 6, *C* and *F*). This suggests that it is the adaptation drift rate, rather than the test drift rate, that produces the changes in the subsequent adaptation accuracy.

The decrease after adaptation at low drift rates is mainly explainable because the slopes of the postadaptation CRFs are slightly shallower than those after adaptation to zero contrasts. The increase in information after high drift rate adaptation is largely the result of the CRFs becoming steeper and the spiking rates (and therefore the variance) smaller after adaptation.

Sources of adaptation effects

A multichannel theory could be used to explain the differences between adaptation properties at low and high drift rates if it is assumed that each cortical neuron receives input from a range of cells with different drift-rate selectivity (also suggested by Maddess et al. 1988). If a multichannel theory is correct, it is unlikely that the different temporal frequency channels would have completely nonoverlapping temporal frequency ranges, so it is to be expected that at least some cross-TF adaptation might occur, as we observed. If a multichannel theory can explain the data, the separate channels most likely arise in the dLGN, which provides the majority of the feedforward drive to the cortex.

The two visual pathways from the dLGN that we know most about are the X- and Y-type cells. Areas 17 and 18 receive input primarily from X- and Y-cells, respectively, but there is also substantial cross talk between cortical areas (for reviews, see Burke et al. 1992; Dreher et al. 1980, 1992; Stone and Dreher 1973). In our experiments, the adapting contrast ranged from 0 to 0.32, the mean peak drift rate was 5.5 Hz, and the mean high adapting drift rate was 13.9 Hz (Fig. 7). Optimal drift rates for X- and Y-cells in cat at a contrast of 0.4 were previously shown to be 4.2 and 5.6 Hz (X and Y, respectively) (Saul and Humphrey 1990). Sclar (1987) showed that temporal frequency tuning in dLGN cells is dependent on contrast. At low contrast levels (0.1), Sclar obtained mean temporal frequency optima for X- and Y-cells that were similar to each other (8.1 and 8.4 Hz, respectively). At high contrast (0.8) the mean peak drift rate for Y-cells increased significantly to 16.8 Hz but increased far less for X-cells (12 Hz). The contrast-dependent changes in the temporal responses of geniculate cells are similar to those observed in retinal ganglion cells (Shapley and Victor 1978).

It was previously shown that some form of contrast adaptation occurs in 46% of X- and Y-type cells in cat dLGN (Shou et al. 1996). For the cat, 8/44 (18%) cells showed contrast gain control in which CRFs moved laterally along the contrast axis. However, these cells were always tested at quite low drift rates (3 Hz). Stronger adaptation was observed in magnocellular cells of the monkey LGN but mainly for high drift rates (usually tested at 11 Hz) (Solomon et al. 2004). We believe that a more extensive survey of contrast adaptation properties in the cat dLGN would reveal powerful contrast gain control at high drift rates. Certainly, the 11 Hz used in the monkey experiments is close to the high drift-rate values used in our experiments. Based on the temporal tuning for dLGN cells, in our experiments it is probable that both X- and Y-cells were adapted equally at peak and high drift rates.

Thus adaptation earlier in the visual pathway might, at least partially, be the source of the high-frequency adaptation effects observed in our cortical data. The drift rates at which cortical cells cease responding are lower than those for LGN cells (e.g., Holub and Morton-Gibson 1981). This is believed to be a result of the low-pass filtering of LGN signals at the thalamocortical

synapse arising from *N*-methyl-D-aspartate–mediated excitatory conductance (Krukowski et al. 2001).

So far we have highlighted the different outcomes of contrast adaptation at low and high drift rates. Our data also show that nonadapted CRFs saturate at higher contrasts when tested with higher drift rates. Several previous authors also demonstrated this effect in cat LGN (Mante et al. 2005) and cat and monkey cortex (Albrecht 1995; Carandini et al. 1997; Hawken et al. 1992; Holub and Morton-Gibson 1981). At first glance, differing contrast functions at different drift rates could provide support for different frequency channels that have different contrast coding properties. However, for cells in macaque V1, this effect has been well accounted for using Heeger's normalization model (Carandini et al. 1997; Heeger 1991, 1992). This model explains the temporal frequency-dependent shift in contrast saturation without need for separate channels. Although this model does not argue directly against the multitemporal-frequency channel theory outlined above, it does show that a multichannel theory is not required to explain differences in nonadapted contrast coding at different drift rates.

ACKNOWLEDGMENTS

Thanks go to Dr. Nicholas Price and S. Wilson for help during recording sessions. Exceptional animal care was provided by K. Debono and K. Wall.

GRANTS

This work was supported by National Health and Medical Research Council Grant 224263 and Australian Research Council Centre for Excellence in Vision Science Grant CE0561903 to M. Ibbotson and National Science and Engineering Research Council of Canada grant to N. Crowder.

REFERENCES

Albrecht DG. Visual cortex neurons in monkey and cat: effect of contrast on the spatial and temporal phase transfer functions. *Vis Neurosci* 12: 1191–1210, 1995.

Albrecht DG, Farrar SB, Hamilton DB. Spatial contrast adaptation characteristics of neurones recorded in the cat's visual cortex. *J Physiol* 347: 713–739, 1984.

Albrecht DG, Geisler WS, Frazor RA, Crane AM. Visual cortex neurons of monkeys and cats: temporal dynamics of the contrast response function. *J Neurophysiol* 88: 888–913, 2002.

Albrecht DG, Hamilton DB. Striate cortex neurons in monkey and cat: contrast response function. *J Neurophysiol* 48: 217–237, 1982.

Attwell D, Laughlin SB. An energy budget for signalling in the grey matter of the brain. *J Cereb Blood Flow Metab* 21: 1133–1145, 2001.

Blakemore C, Muncey JPJ, Ridley RM. Stimulus specificity in the human visual system. *Vision Res* 13: 1915–1931, 1973.

Bonds AB. Temporal dynamics of contrast gain in single cells of the cat striate cortex. *Vis Neurosci* 6: 239–255, 1991.

Burke W, Dreher B, Michalski A, Cleland BG, Rowe MH. Effects of selective pressure block of Y-type optic nerve fibers on the receptive-field properties of neurons in the striate cortex of the cat. *Vis Neurosci* 9: 47–64, 1992.

Butts DA, Goldman MS. Tuning curves, neuronal variability, and sensory coding. *PLoS Biol* 4: e92, 2006.

Carandini M, Ferster D. A tonic hyperpolarization underlying contrast adaptation in cat visual cortex. *Science* 276: 949–952, 1997.

Carandini M, Heeger DJ, Movshon JA. Linearity and normalization in simple cells of the macaque primary visual cortex. *J Neurosci* 17: 8621–8644, 1997.

Chirimuuta M, Clatworthy PL, Tolhurst DJ. Coding of the contrasts in natural images by visual cortex (V1) neurons: a Bayesian approach. *J Opt Soc Am A* 20: 1253–1260, 2003.

Clifford CWG, Ibbotson MR. Response variability and information transfer in directional neurons of the mammalian horizontal optokinetic system. *Vis Neurosci* 17: 207–215, 2000.

Clifford CWG, Ibbotson MR. Fundamental mechanisms of visual motion detection: models, cells and functions. *Prog Neurobiol* 68: 409–437, 2002.

Crowder NA, Price NS, Hietanen MA, Dreher B, Clifford CW, Ibbotson MR. Relationship between contrast adaptation and orientation tuning in V1 and V2 of cat visual cortex. *J Neurophysiol* 95: 271–283, 2006.

Dean I, Harper NS, McAlpine D. Neural population coding of sound level adapts to stimulus statistics. *Nat Neurosci* 8: 1684–1689, 2005.

Dragoi V, Sharma J, Sur M. Adaptation-induced plasticity of orientation tuning in adult visual cortex. *Neuron* 28: 287–298, 2000.

Dreher B, Leventhal AG, Hale PT. Geniculate input to cat visual cortex: a comparison of area 19 with areas 17 and 18. *J Neurophysiol* 44: 804–826, 1980.

Dreher B, Michalski A, Cleland BG, Burke W. Effects of selective pressure block of Y-type optic nerve fibers on the receptive-field properties of neurons in area 18 of the visual cortex of the cat. *Vis Neurosci* 9: 65–78, 1992.

Hawken MJ, Shapley RM, Grosof DH. Temporal frequency tuning of neurons in macaque V1: effects of luminance contrast and chromaticity. *Invest Ophthalmol Vis Sci Suppl* 33: 955, 1992.

Heeger DJ. Nonlinear model of neural responses in cat visual cortex. In: *Computational Models of Visual Processing*, edited by Landy M, Movshon JA. Cambridge, MA: MIT Press, 1991, p. 119–133.

Heeger DJ. Normalization of cell responses in cat striate cortex. *Vis Neurosci* 9: 181–198, 1992.

Holub RA, Morton-Gibson M. Response of visual cortical neurons of the cat to moving sinusoidal gratings: response-contrast functions and spatiotemporal interactions. *J Neurophysiol* 46: 1244–1259, 1981.

Hubel DH, Wiesel TN. Receptive fields, binocular interaction and functional architecture in the cat's visual cortex. *J Physiol* 160: 106–154, 1962.

Ibbotson MR. Physiological mechanisms of adaptation in the visual system. In: *Fitting the Mind to the World: Adaptation and Aftereffects in High-Level Vision*, edited by Clifford C, Rhodes G. Oxford, UK: Oxford Univ. Press, 2005a, p. 17–45.

Ibbotson MR. Contrast and speed related gain control in the pretectal nucleus of the optic tract. *J Neurophysiol* 94: 136–146, 2005b.

Ibbotson MR, Price NSC, Crowder NA. On the division of cortical cells into simple and complex types: a comparative viewpoint. *J Neurophysiol* 93: 3699–3702, 2005.

Kohn A, Smith MA. Stimulus dependence of neuronal correlation in primary visual cortex of the macaque. *J Neurosci* 25: 3661–3673, 2005.

Krukowski AE, Troyer TW, Miller KD. A model of visual cortical temporal frequency tuning. *Neurocomputing* 38–40: 1379–1383, 2001.

Lennie P. The cost of cortical computation. *Curr Biol* 13: 493–497, 2003.

Maddess T, McCourt ME, Blakeslee B, Cunningham RB. Factors governing the adaptation of cells in area-17 of the cat visual cortex. *Biol Cybern* 59: 229–236, 1988.

Mante V, Frazor RA, Bonin V, Geisler WS, Carandini M. Independence of luminance and contrast in natural scenes and in the early visual system. *Nat Neurosci* 12: 1690–1697, 2005.

Movshon JA, Lennie P. Pattern-selective adaptation in visual cortical neurones. *Nature* 278: 850–852, 1979.

Movshon JA, Thompson ID, Tolhurst DJ. Spatial and temporal contrast sensitivity of neurones in areas 17 and 18 of the cat visual cortex. *J Physiol* 283: 101–120, 1977.

Müller JR, Metha AB, Krauskopf J, Lennie P. Rapid adaptation in visual cortex to the structure of images. *Science* 285: 1405–1408, 1999.

Nover H, Anderson CH, DeAngelis GC. A logarithmic, scale-invariant representation of speed in macaque middle temporal area accounts for speed discrimination performance. *J Neurosci* 25: 10049–10060, 2005.

Ohzawa I, Sclar G, Freeman RD. Contrast gain control in the cat's visual system. *J Neurophysiol* 54: 651–667, 1985.

Pouget A, Zhang K, Deneve S, Latham PE. Statistically efficient estimation using population coding. *Neural Comput* 10: 373–401, 1998.

Price NS, Crowder NA, Hietanen MA, Ibbotson MR. Neurons in V1, V2, and PMLS of cat cortex are speed tuned but not acceleration tuned: the influence of motion adaptation. *J Neurophysiol* 95: 660–673, 2006.

Saul AB, Cynader MS. Adaptation in single units in visual cortex: the tuning of motion aftereffects in the spatial domain. *Vis Neurosci* 2: 593–607, 1989a.

Saul AB, Cynader MS. Adaptation in single units in visual cortex: the tuning of motion aftereffects in the temporal domain. *Vis Neurosci* 2: 609–620, 1989b.

Saul AB, Humphrey AL. Spatial and temporal response properties of lagged and nonlagged cells in cat lateral geniculate nucleus. *J Neurophysiol* 64: 206–224, 1990.

Sclar G. Expression of "retinal" contrast gain control by neurons of the cat's lateral geniculate nucleus. *Exp Brain Res* 66: 589–596, 1987.

Sclar G, Lennie P, DePriest DD. Contrast adaptation in striate cortex of macaque. *Vision Res* 29: 747–755, 1989.

Seung HS, Sompolinsky H. Simple models for reading neuronal population codes. *Proc Natl Acad Sci USA* 90: 10749–10753, 1993.

Shadlen MN, Newsome WT. The variable discharge of cortical neurons: implications for connectivity, computation, and information coding. *J Neurosci* 18: 3870–3896, 1998.

Shapley RM, Victor JD. The effect of contrast on the transfer properties of cat retinal ganglion cells. *J Physiol* 285: 275–298, 1978.

Shou T, Li X, Zhou Y, Hu B. Adaptation of visually evoked responses of relay cells in the dorsal lateral geniculate nucleus of the cat following prolonged exposure to drifting gratings. *Vis Neurosci* 13: 605–613, 1996.

Snowden RJ, Hammett ST. Spatial frequency adaptation: threshold elevation and perceived contrast, *Vision Res* 32: 1797–1809, 1996.

Solomon SG, Peirce JW, Dhruv NT, Lennie P. Profound contrast adaptation early in the visual pathway. *Neuron* 42: 155–162, 2004.

Stone J, Dreher B. Projection of X- and Y-cells of the cat's lateral geniculate nucleus to areas 17 and 18 of visual cortex. *J Neurophysiol* 40: 1051–1065, 1973.

Tolhurst DJ, Movshon JA, Thompson ID. The dependence of response amplitude and variance of cat visual cortical neurons on stimulus contrast. *Exp Brain Res* 42: 414–419, 1981.

Zohary E, Shadlen MN, Newsome WT. Correlated neuronal discharge rate and its implications for psychophysical performance. *Nature* 370: 140–143, 1994.